



**HAL**  
open science

## Pattern Reconfigurable Cubic Antenna

Julien Sarrazin, Yann Mahé, Stéphane Avrillon, Serge Toutain

► **To cite this version:**

Julien Sarrazin, Yann Mahé, Stéphane Avrillon, Serge Toutain. Pattern Reconfigurable Cubic Antenna. IEEE Transactions on Antennas and Propagation, 2009, 57 (2), pp.310 - 317. 10.1109/TAP.2008.2011221 . hal-00949549

**HAL Id: hal-00949549**

**<https://hal.science/hal-00949549v1>**

Submitted on 21 Feb 2014

**HAL** is a multi-disciplinary open access archive for the deposit and dissemination of scientific research documents, whether they are published or not. The documents may come from teaching and research institutions in France or abroad, or from public or private research centers.

L'archive ouverte pluridisciplinaire **HAL**, est destinée au dépôt et à la diffusion de documents scientifiques de niveau recherche, publiés ou non, émanant des établissements d'enseignement et de recherche français ou étrangers, des laboratoires publics ou privés.

# Pattern Reconfigurable Cubic Antenna

Julien Sarrazin<sup>(1)</sup>, *Student Member, IEEE*, Yann Mahé<sup>(1)</sup>, Stéphane Avrillon<sup>(2)</sup>, *Member, IEEE*,  
and Serge Toutain<sup>(1)</sup>

<sup>(1)</sup> Institut de Recherche en Electrotechnique et Electronique de Nantes Atlantique (IREENA), University of Nantes, France

<sup>(2)</sup> Institut d'Electronique et Télécommunications de Rennes (IETR), University of Rennes, France

***Abstract***-A new single-feed reconfigurable antenna for pattern diversity is presented in this paper. The proposed structure is based on a metallic cubic cavity which radiates through rectangular slots. The pattern reconfiguration is achieved with PIN diode switches by short-circuiting slots in their center. The designed antenna can switch between three different radiation patterns which radiate in a  $4\pi$  steradian range and can receive any incident field polarizations. A prototype of the antenna, including PIN diodes and operating in the 5 GHz band, has been built to demonstrate the feasibility of the concept. Measurements have been conducted and three-dimensional radiation patterns are provided. Diversity performances are evaluated by calculating the envelope correlation coefficient.

***Index Terms***-Reconfigurable antennas, pattern diversity, envelope correlation coefficient, slots and cavity, PIN diode switches

## I. INTRODUCTION

**D**IVERSITY antenna systems are widely used in order to increase wireless communication data rates [1]. With multiple antennas receiving uncorrelated signals, it is possible to avoid fading effects and to obtain a better transmission quality. Many techniques exist to maximize the Signal-to-Noise Ratio (SNR). Some of them combine received signals from each antenna (equal gain, maximal ratio combining, etc...) and others select the best received signal from multiple antennas (selection diversity, switched diversity, etc...). The switched diversity has the advantage of needing only one switched access for all antennas. Therefore, only one front-end is required. Diversity performances depend on the correlation

between each received signal. For a spatial diversity scheme, the signal decorrelation is achieved by a large space (compared to the wavelength) between each antenna. However, such a solution cannot always be used in relation with the limited volume available on a communicating terminal. Then radiation and/or polarization diversities can replace spatial diversity to respect the limited dimensions of the terminal [2]-[7]. Furthermore, in one-access diversity schemes like switched diversity, instead of using many antennas which radiate with different patterns or polarizations, another solution is to use reconfigurable antennas [8]. If available patterns on these antennas provide uncorrelated received signals, high diversity performances can be obtained.

More recently, reconfigurable antennas regained a new research interest with Multiple Input Multiple Output (MIMO) systems. These systems use multiple antennas at both the receiver and the transmitter in order to increase communication capacity. Generally, the higher the number of antennas, the better the capacity enhancement. However, their radiation characteristics also have an important impact on the channel capacity [9]. Antenna patterns which offer low signal correlation between each radiating element are suitable for a high channel capacity. Furthermore, since the channel is not stationary, it is interesting that each antenna of the MIMO system can switch between different radiation pattern configurations in order to optimize, in real time, the channel capacity to prevent environment modifications. Consequently, a reconfigurable antenna used as one of multiple radiating elements offers an additional degree of freedom for adaptive MIMO communications [10]-[13].

Diversity antenna communications are often used in urban or indoor environments where multipath effects are strong. Therefore, our work focuses on developing antennas which radiate in a  $4\pi$  steradian range so as to be able to receive signals coming from many directions. The severe fading effects of scattering environments can be avoided by the proposed antenna design, which is sensitive to three orthogonal polarizations. By using PIN diodes, the reconfigurable antenna allows switching between three different radiation patterns which provide uncorrelated signals [14]. The design and mechanism of the proposed pattern reconfigurable cubic antenna are described in Section II. More details on how the reconfiguration has been done in practice are given in Section III where measurements are also presented. Diversity performances of the structure are discussed in Section IV by calculating envelope correlations.

## II. RECONFIGURABLE CUBIC ANTENNA ANALYSIS

### A. Antenna overview

Fig. 1 shows the design of the proposed reconfigurable antenna. Based on a metallic cubic cavity, this structure is fed by a probe penetrating through one cube corner. The radiation is achieved through the 6 slots etched on the 6 cube sides (one per side) which enable the radiation in a  $4\pi$  steradian range. Adjacent slots of the structure are located orthogonally ( $\text{slot}_1 \perp \text{slot}_2, \text{slot}_2 \perp \text{slot}_3, \dots$ ). Thus, since rectangular apertures generate a linear polarization (see arrows on Fig. 1), the radiated electric field is the sum of three orthogonal polarizations for every given direction of propagation. Thereby the structure is sensitive to both polarizations along  $\theta$  and along  $\varphi$  (on spherical coordinates) which is well suited to avoid the propagation fading effects and to maximize the received power. The radiation pattern reconfiguration is achieved by switches located in the middle of each slot. In the ON state, switches act like short-circuits which avoid the radiation through slots whereas in the OFF state, radiation through the slots is possible.

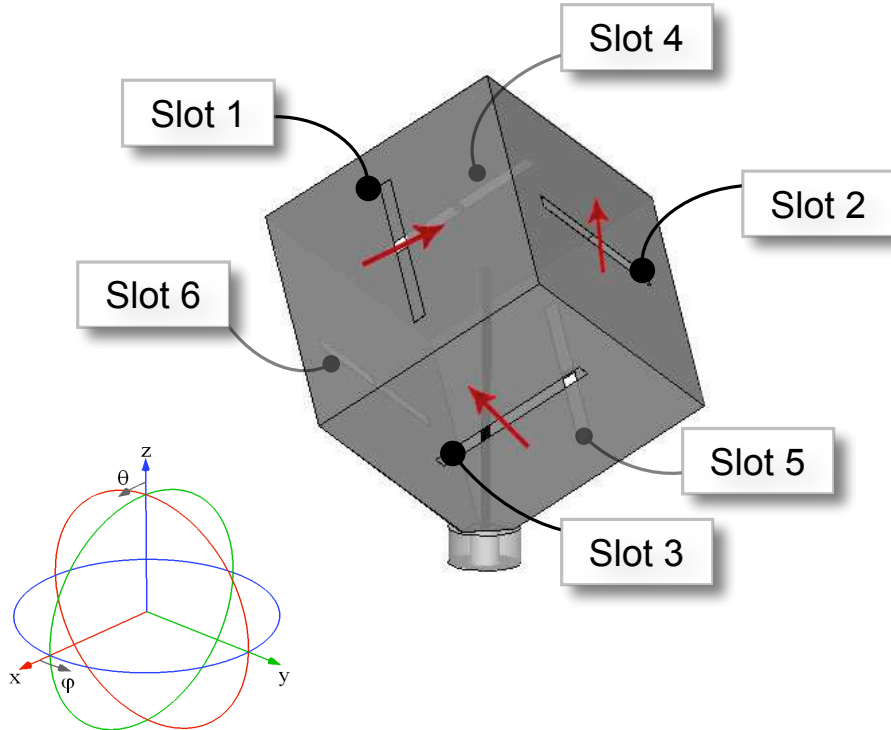


Fig. 1 - Schematic drawing for the reconfigurable cubic antenna

## B. Design concept

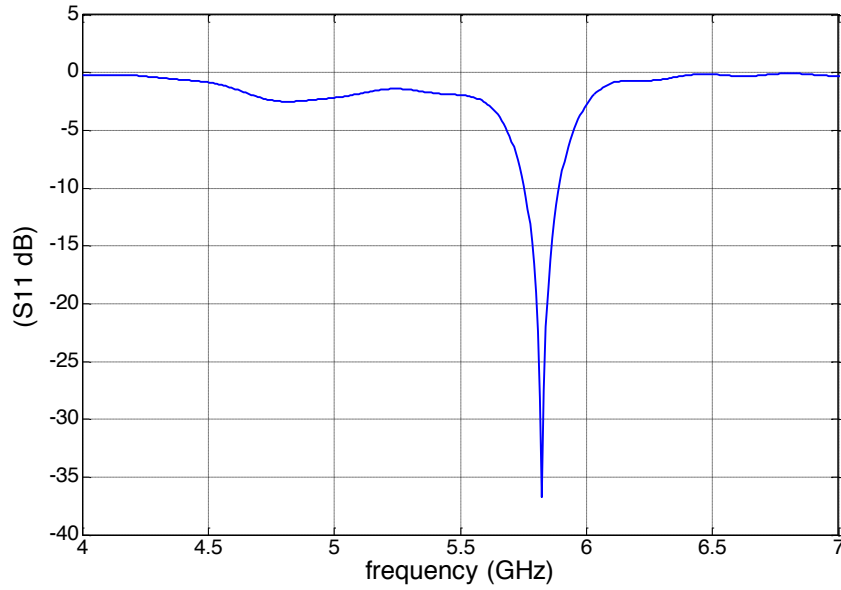
Performances of such a structure are determined by two resonance phenomena. The first one is due to the modes resonating inside the cavity and radiating through the slots. The second one is the slot resonance. By adjusting the probe length, a good impedance matching can be achieved either on the cavity resonance or on the slot resonance.

In the cavity resonance case, the probe feeds the first three orthogonal modes inside the cavity ( $m = n = 1$ ,  $m = p = 1$  and  $n = p = 1$  in equation (1)). Since the cavity is cubic, each mode has the same resonance frequency which can be determined by the following relation:

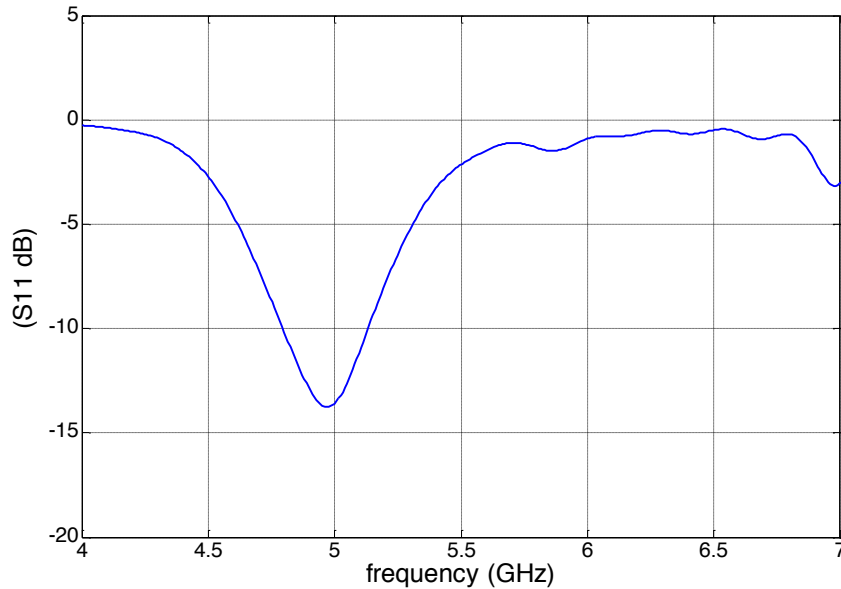
$$f_{mnp} = c \left[ \left( \frac{m}{2a} \right)^2 + \left( \frac{n}{2b} \right)^2 + \left( \frac{p}{2l} \right)^2 \right]^{\frac{1}{2}} = \frac{c}{2a} \sqrt{m^2 + n^2 + p^2}, \quad (1)$$

with  $c$ , the velocity of light,  $a$ ,  $b$ ,  $l$ , the rectangular cavity dimensions, and  $m$ ,  $n$ ,  $p$ , the modal order indexes. Since adjacent slots are orthogonal, each mode can be coupled to only two slots (face to face). The reactive slot effect decreases the cavity resonance frequency and the larger the slot length, the lower the cavity resonance frequency. On the other hand, the probe increases the resonance frequency by adding a capacitive effect.

Taking both of these effects into account, the cube dimension  $a$  can be chosen to work at its first fundamental modes:  $TE_{011}$ ,  $TE_{101}$  and  $TE_{110}$ . A good impedance matching can be achieved by adjusting the probe length. A simulation has been done with the following dimensions:  $a = 37.5$  mm,  $l_s = 27$  mm for the slot length (width = 2 mm) and  $l_p = 28$  mm for the probe length (all the simulations presented in this paper have been done with Ansoft HFSS). Switches for radiation pattern reconfiguration are assumed to be perfect short-circuits in the ON state and perfect open-circuits in the OFF state. The simulated reflection coefficient is shown in Fig. 2 (a). The resonance frequency is about 5.8 GHz. The -10 dB bandwidth is about 2.5% which is a typical value for a cavity resonance (for L- and C-bands).



(a)



(b)

**Fig. 2 - Simulated reflection coefficient of the cubic antenna matched on (a) cavity resonance. (b) slot resonance.**

Another design solution is to use slot resonance instead of cavity resonance by coupling energy directly from the probe to the slots. Keeping the cube sizes identical ( $a = 37.5$  mm and  $l_s = 27$  mm) and changing only the probe length, it is possible to match the slot resonance of the antenna which occurs at a lower frequency. In this case, the probe length has been increased up to  $l_p = 44$  mm.

Reflection coefficient presented in Fig. 2 (b) shows that slots resonate at 5 GHz. The -10 dB bandwidth is about 6.5% which is wider than the cavity resonance case.

It is interesting to take advantage of the multi-resonant behavior of this structure in order to increase the frequency bandwidth in which such an antenna can operate. In fact, by a judicious design, it is possible to overlay the two resonances involved. Antenna dimensions have been changed in order to bring the cavity and slot resonance frequencies closer together. With the following dimensions:  $a = 39.5$  mm,  $l_s = 27$  mm,  $l_p = 38$  mm, slot and cavity resonances are coupled and cause two resonances at 5.05 GHz and at 5.4 GHz. So, the impedance matching is achieved over the two resonances as it is shown in Fig. 3. Thus, the -10 dB bandwidth has been increased up to 11.3% around 5.2 GHz.

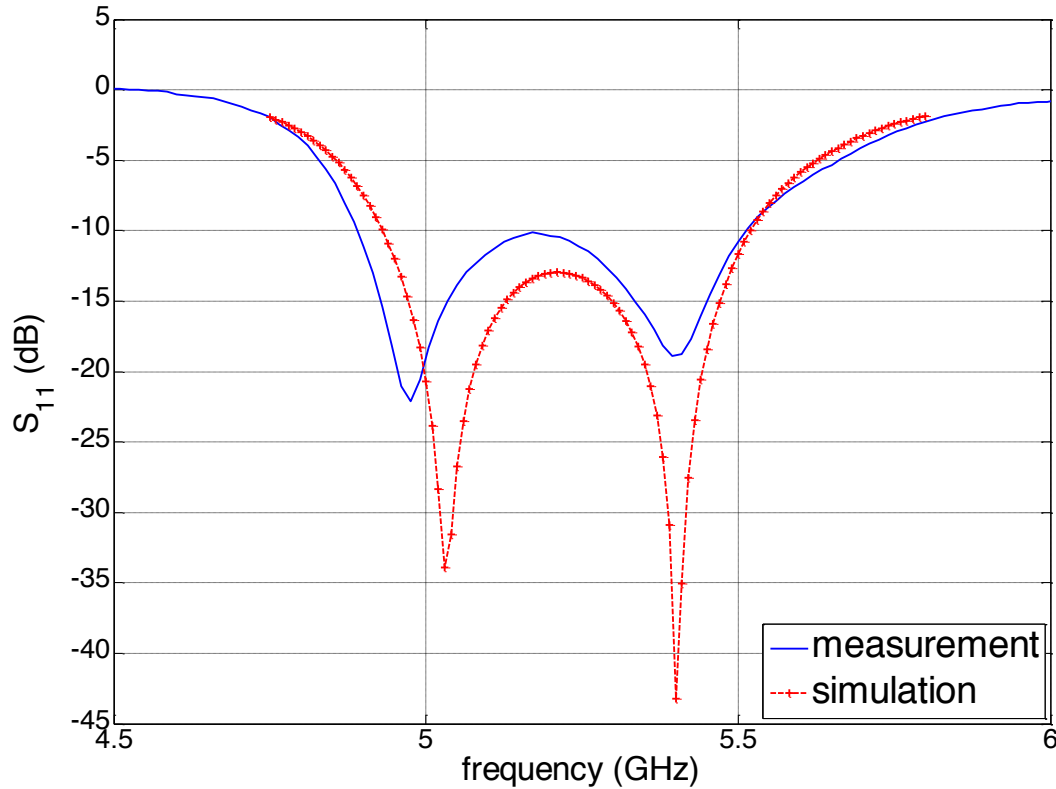


**Fig. 3 - Comparison of simulated and measured reflection coefficient for the dual-resonance antenna**

A prototype has been created to validate the concept experimentally. A picture is shown in Fig. 4. The cavity is made with brass. As in the previous simulations, short-circuits are supposed ideal and are made with metallic tape. The measurement of the antenna reflection coefficient is compared to the simulation in Fig. 3. A -10 dB bandwidth about 11.9% is achieved around 5.2 GHz which is in good agreement with the simulation results.

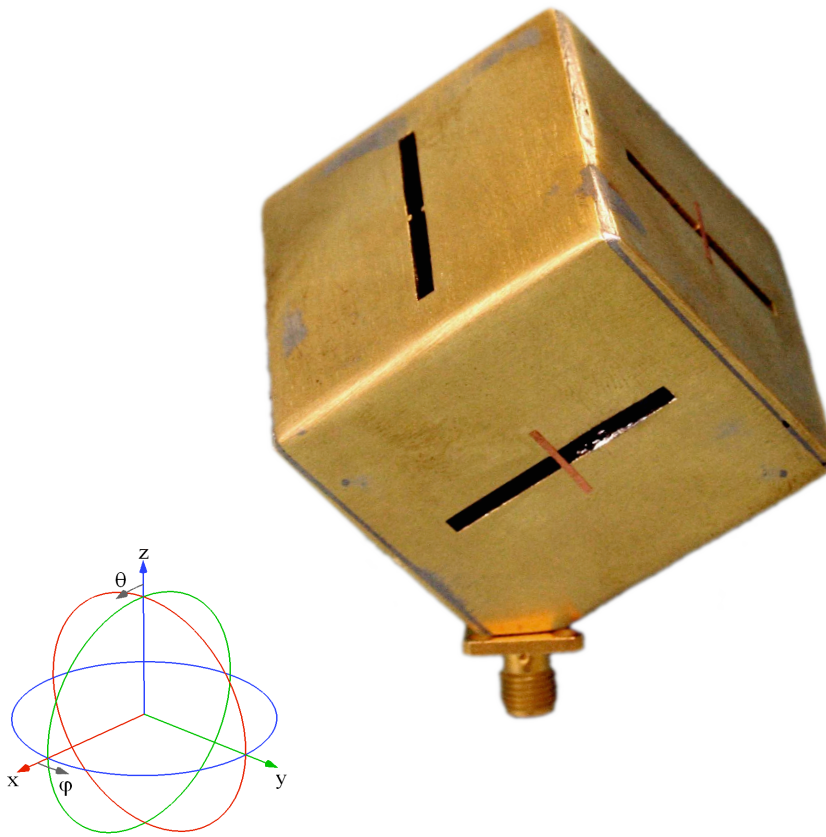


**Fig. 4 – Built cubic antenna**

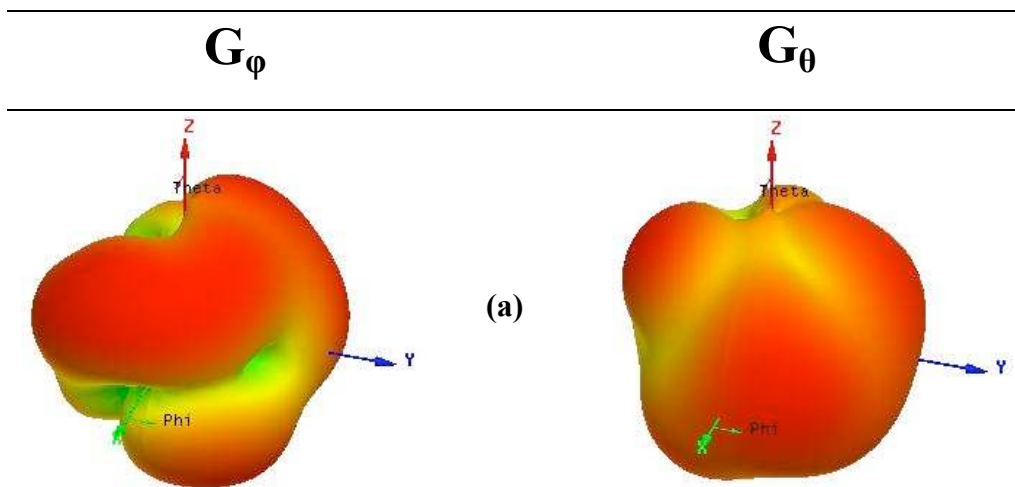
### *C. Pattern reconfiguration*

The pattern reconfiguration is achieved by short-circuiting slots in their center to cancel their radiation contribution. This action can be done by PIN diodes for example. The switch in the OFF state (open-circuit) allows the radiation through the corresponding slot whereas the switch in the ON state (short-circuit) cancels the radiation and the slot can be considered a metallic wall. Since every slot can radiate or not depending on the state of the switches, pattern reconfiguration is achieved by selecting which slots are short-circuited. Three interesting configurations have been studied because of their high pattern diversity in a  $4\pi$  steradians environment. Each one contains two short-circuited slots on the lower sides and one on the upper as indicated in Table 1 (slot numbers refer to Fig. 1). Switching configuration is equivalent to rotating the cube around the probe on a  $120^\circ$  angle. Thus, the antenna reflection coefficient is not affected by the change of configuration.

Configuration	Radiated slots	Short-circuited slots
1	Slot 1, slot 2, slot 3	Slot 4, slot 5, slot 6
2	Slot 2, slot 4, slot 5	Slot 1, slot 3, slot 6
3	Slot 1, slot 4, slot 6	Slot 2, slot 3, slot 5

**Table 1 - Switches configurations**

The cubic antenna with the previous given dimensions (the cube which uses slot and cavity resonances) has been simulated and radiation patterns for the three configurations are drawn in Fig. 5. Since the radiation is quite constant on the whole frequency band, only results at 5.4 GHz are shown here. Radiation patterns are drawn along spherical coordinates  $\theta$  and  $\varphi$ . The gain  $\theta$  is defined using the electric field projection on the vector  $u_\theta$  and the gain  $\varphi$  using the projection on the vector  $u_\varphi$ . Each configuration provides the same shape but rotated on a  $120^\circ$  angle. One can notice that the structure radiates in a  $4\pi$  steradian range with some maximum gain directions. Depending on the chosen configuration, the antenna radiates through different slots and accordingly, maximum gain directions change. Hence radiation pattern diversity in power is achieved. Maximum gain values along  $\theta$  and  $\varphi$  are both approximately equal to 3.7 dBi which confirms that the antenna is sensitive to both polarizations (along  $\theta$  and along  $\varphi$ ). Furthermore, in a given direction of propagation, the radiated power along  $\theta$  and along  $\varphi$  are not respectively identical depending on which configuration the antenna is set: the ratio  $G_\varphi/G_\theta$  can be higher or lower than one. So, radiation pattern diversity in polarization is also achieved. Switching configuration provides diversity with all radiation properties: power, phase (not represented here) and polarization.



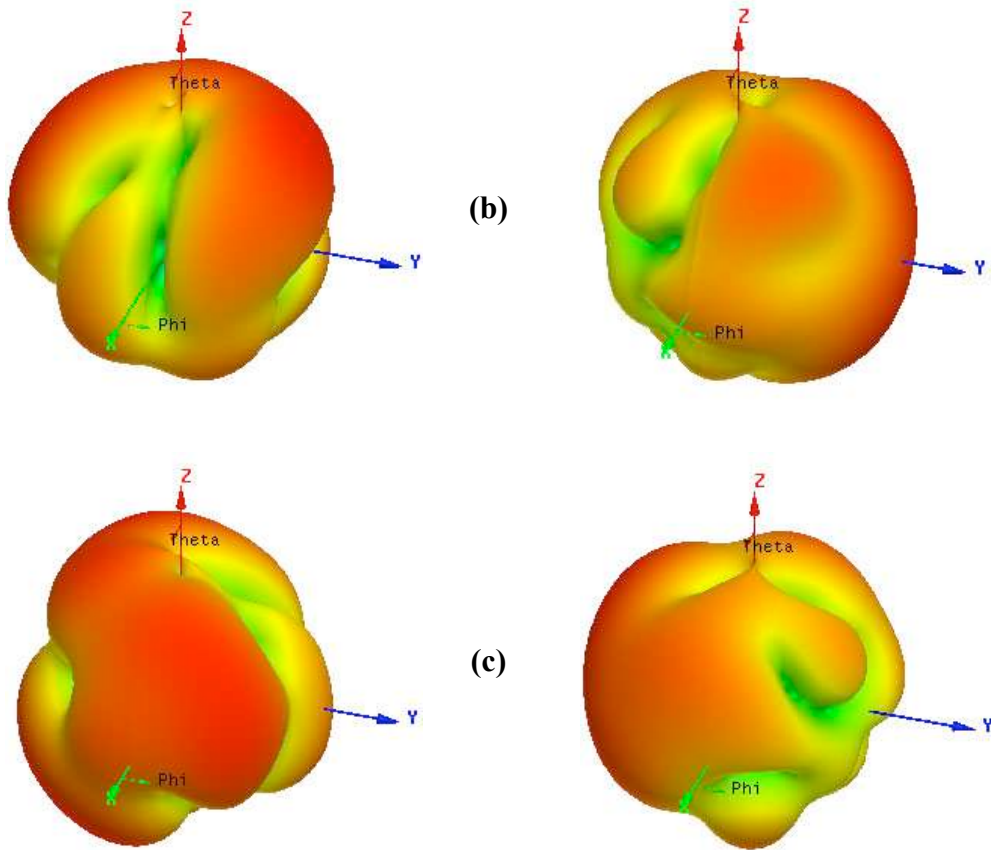


**Fig. 5 - Simulated radiation patterns along  $\phi$  (on left) and  $\theta$  (on right) for (a) configuration 1, (b) configuration 2 and (c) configuration 3**

### III. RADIATION PATTERN RECONFIGURATION WITH PIN DIODES

After studying the cubic antenna with “hard-wired” switches, this section focuses on the use of PIN diodes to control the radiation pattern with a simple binary command. Since diodes must act as short-circuits on the slots etched on the metallic sides of the cube, precautions have to be taken for the DC bias: one of the pins of each diode has to be isolated. That is why a thin dielectric sheet of teflon (200  $\mu\text{m}$ ) is inserted between the diode and the metallic cube side as shown in Fig. 6. The teflon forms a rectangle of about 6x7 mm<sup>2</sup> in order to create a capacitance under one of diode pins. This capacitance allows the transmission of high frequency signals while stopping DC potentials. Thus, teflon capacitance combined with diodes in the ON state are seen as a short-circuit in high frequencies. The teflon is metal-coated to easily weld to the diode pin. A thin teflon line, which is also metal-coated, joins this capacitance to a little pad down the cube. Thus, by welding bias wires on the six little pads (one per diode), it is possible to control diode states by applying a DC potential of about one

volt. The DC ground is taken with a wire welded directly on the cubic cavity. Since the DC potential does not propagate on the same conductor as the high frequency signal, no DC blocker is needed. Bias lines are pasted on the surface cube as far as possible from the slots in order to disturb the radiation as little as possible.

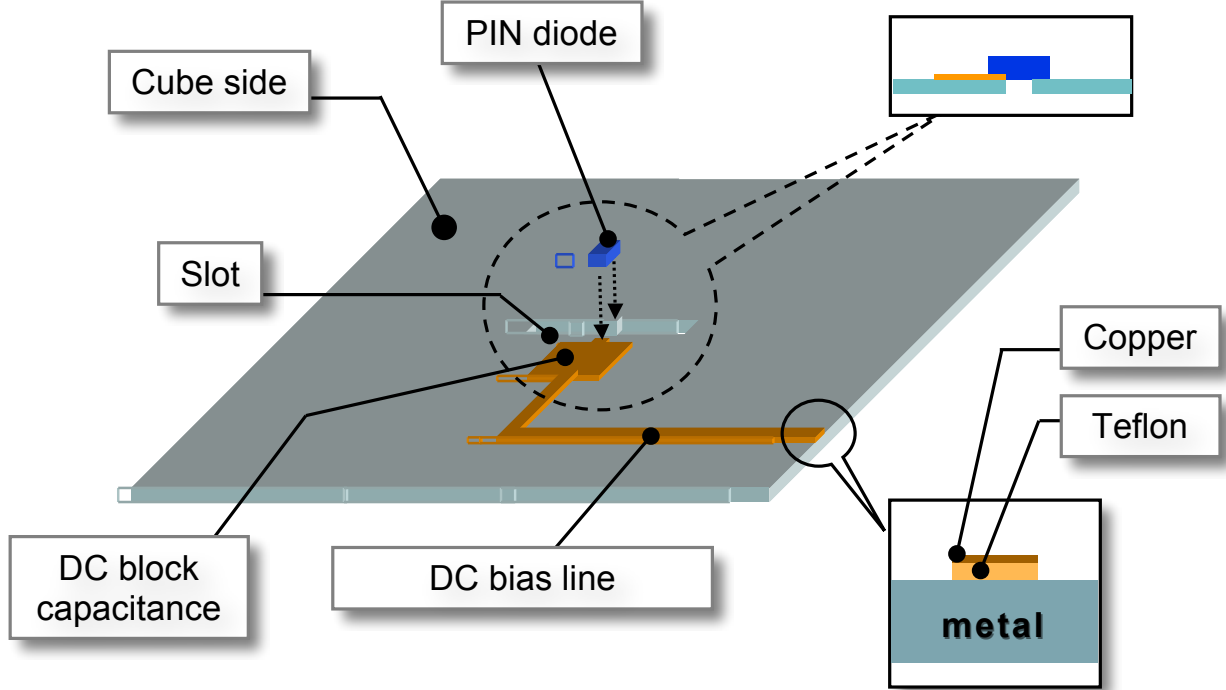
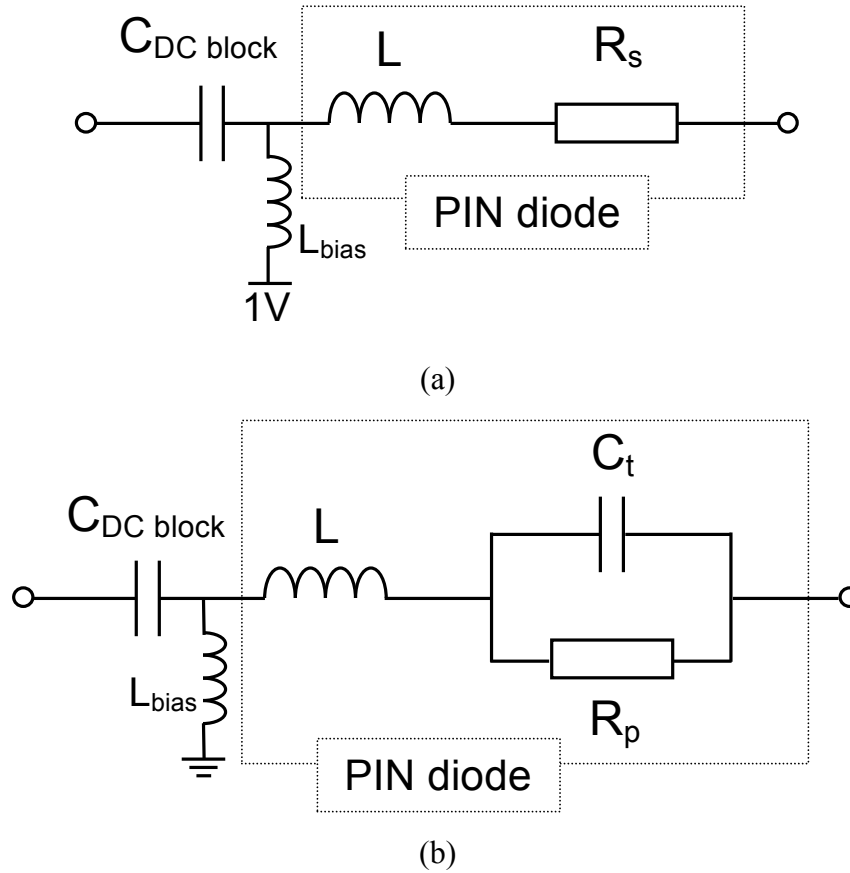


Fig. 6 - PIN diode location on a cube side with DC bias circuit

Since the bias circuit is outside the cavity, it has no impact on the resonant behavior of the structure. Only the diodes with their DC block capacitances have an impact on the antenna resonance frequency. In fact, the reactive effect involved decreases the resonance frequency of the slots whereas this effect is not significant on the cavity resonance.

In order to better understand diode influences, simulations have been done with the RF equivalent circuit of the realistic switches instead of the “hard-wired” switches. The equivalent circuit introduced in the simulation software is presented in Fig. 7. This circuit includes both the DC block capacitance and the PIN diode in (a) the ON state and in (b) the OFF state. Since the bias line is thin, it can be modelled by an inductance  $L_{bias}$ . At operating frequency, it can be assumed that its impedance ( $\sim jL_{bias}\omega$ ) is very high, so its effect can be neglected in the equivalent circuit. Component values related to the diode are given by the constructor and are:  $L = 0.6$  nH,  $R_S = 40$   $\Omega$ ,  $C_T = 0.15$  pF and  $R_P = 5$  k $\Omega$ . The DC block capacitance can be determined with the expression:  $C = \epsilon_0 \epsilon_r \frac{S}{e}$ , where  $\epsilon_0$  is the permittivity of free space,  $\epsilon_r = 2.55$  is the relative permittivity of the Teflon substrate,  $S = 42$  mm<sup>2</sup> is the

capacitance surface and  $e = 200 \mu\text{m}$  is the substrate thickness. So the DC block capacitance value is  $C_{DC\ block} = 4.74 \text{ pF}$ .



**Fig. 7 – RF equivalent circuit for PIN diode and DC block capacitance in the (a) ON state (forward bias) and (b) OFF state (reverse bias)**

Since diode effects are not identical on the cavity resonance with that of the slot resonance, it is not possible to achieve a matching over the two resonances anymore while keeping the same antenna dimensions as previously. The simulated reflection coefficient of the antenna with the previous dimensions ( $a = 39.5 \text{ mm}$ ,  $l_s = 27 \text{ mm}$ ,  $l_p = 38 \text{ mm}$ ) including switch equivalent circuits in the ON and OFF states is given in Fig. 8. Even if cavity and slot resonances can be distinguished, a -10 dB matching is not achieved. By adjusting the probe length  $l_p$ , it is possible to match the antenna either to the cavity resonance with  $l_p = 17 \text{ mm}$  or to the slot resonance with  $l_p = 59.3 \text{ mm}$  as shown in Fig. 8. The cavity resonance occurs at 5.38 GHz whereas the slot resonance occurs at 3.85 GHz. We note that the cavity resonance frequency does not shift. The simulation shows that the switch behavior on the antenna structure has no impact on the cavity resonance frequency but shifts the slot resonance frequency. The equivalent circuit of the diode in the OFF state and the DC block capacitance introduces a reactive effect on radiated slots which decrease their resonance frequency from about 5 GHz down to 3.85 GHz. So, the gap between resonance frequencies of slots and

cavity becomes too large to match the antenna over the two resonances simultaneously. A solution to overcome this problem is to reduce the slot length in order to increase its resonance frequency. With a slot length of  $l_s = 15$  mm instead of 27 mm and a probe length of  $l_p = 34$  mm, slots and cavity resonate at frequencies close enough to match the antenna over the two resonances as shown in Fig. 9. However, with the diode equivalent circuits, the bandwidth is now about 5.6 %, which is narrower than the 11.3 % bandwidth obtained by the simulation with “hard-wired” switches. Diodes introduce a reactive effect which increases the Q-factor of slot resonators. The individual frequency bandwidth of radiated slots becomes narrower. So, cavity and slot resonances have to be closer in order to be coupled. This explains why the whole bandwidth of the antenna with realistic switches instead of “hard-wired” switches is narrower.

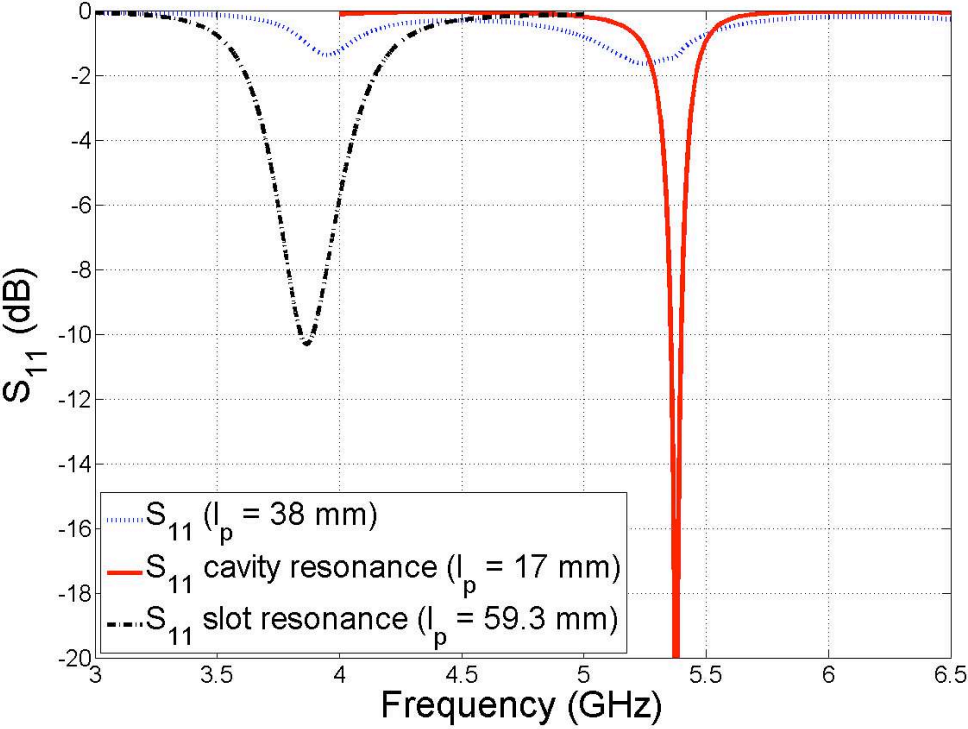


**Fig. 8 - Simulated reflection coefficient including switch equivalent circuits**

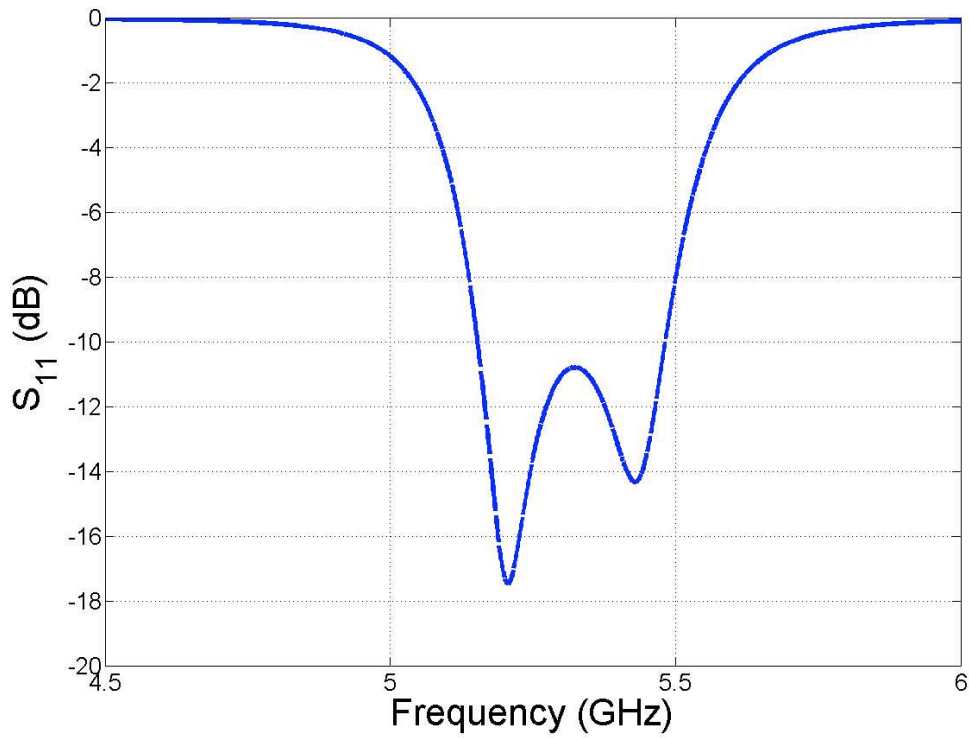


**Fig. 9 - Simulated reflection coefficient with adjusted probe length**

The antenna with PIN diodes and the bias circuit has been built and is shown in Fig. 10. Bias wires are all connected to the structure near the RF coaxial connector. Measurements have been done for the three expected configurations. Each one contains three diodes in the ON state and three in the OFF state as in the previous section, but this time with PIN diodes instead of “hard-wired” switches.

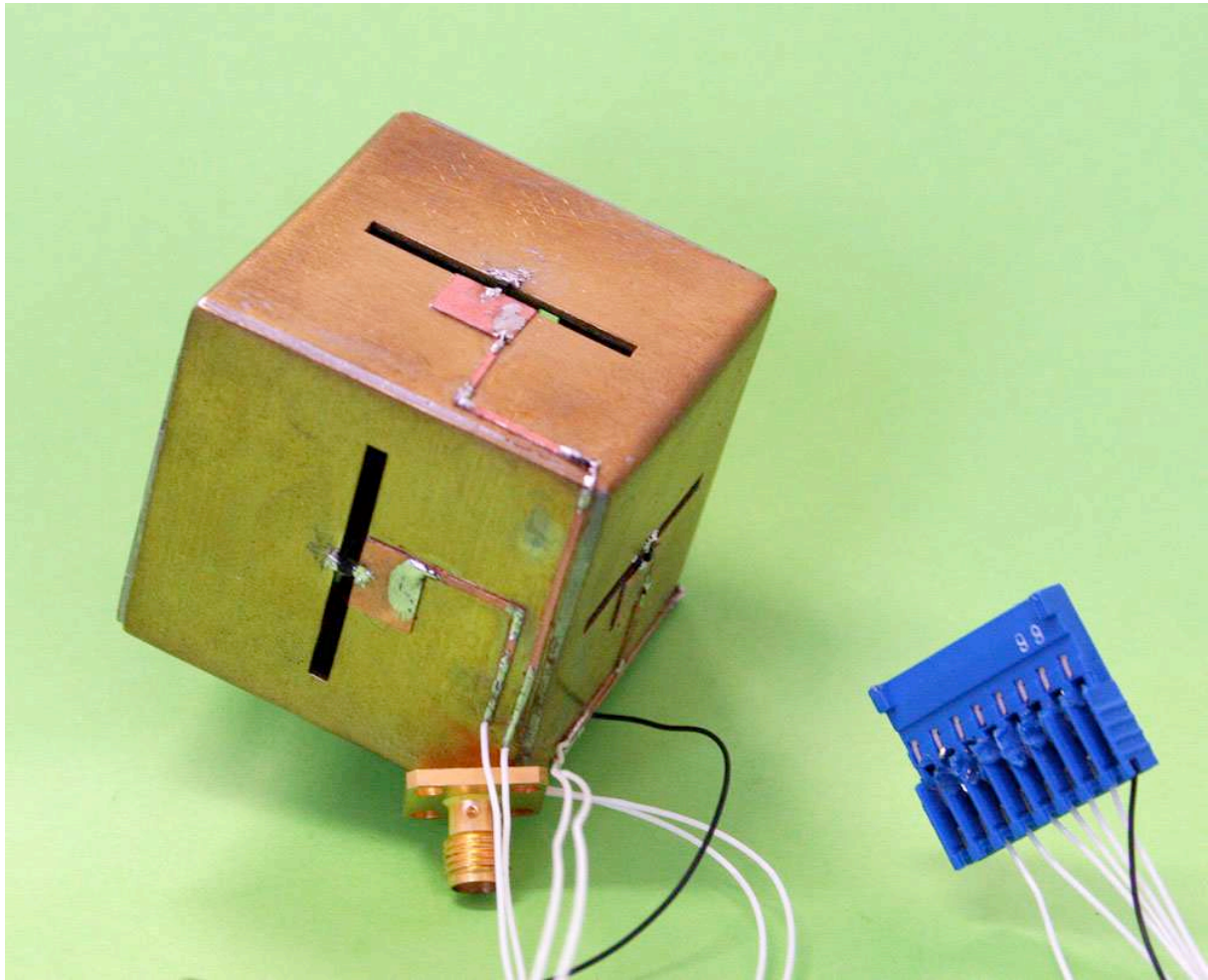


**Fig. 10 - Picture of the reconfigurable cubic antenna**

Fig. 11 shows the measured reflection coefficient for the three pattern configurations. A good impedance matching is achieved around 5.2 GHz in the three cases. The -10 dB frequency bandwidths go from 5.4% for the configuration 2 up to 8.8% for the configuration 1. By considering the three configurations, a -10 dB shared bandwidth of 285 MHz is available between 5.025 GHz and 5.31 GHz. Cavity and slot resonances are easily detectable especially in the configuration 1. Differences between each configuration are due to the fact that the feeding probe which penetrates through one cube corner has not been perfectly located during the construction. Inside the cavity, the probe is a little bit deviated from the main cube axis and, consequently, is nearer to some slots than from others. So the quantity of the coupled energy is not the same depending on which slot is considered. Another imperfection in the actual construction is the isolation capacitance sizes which are not strictly identical on every cube side. Thus reactive effects induced by these capacitances on each slot are not exactly equal and so neither are the slots resonance frequencies. These frequency shifts can also explain the impedance matching level differences between each configuration:

since all configurations are not identical, the probe length is inevitably better optimized for one configuration than others. A better agreement between simulation and measurement could be obtained by a prototype fabricated with an industrial process.

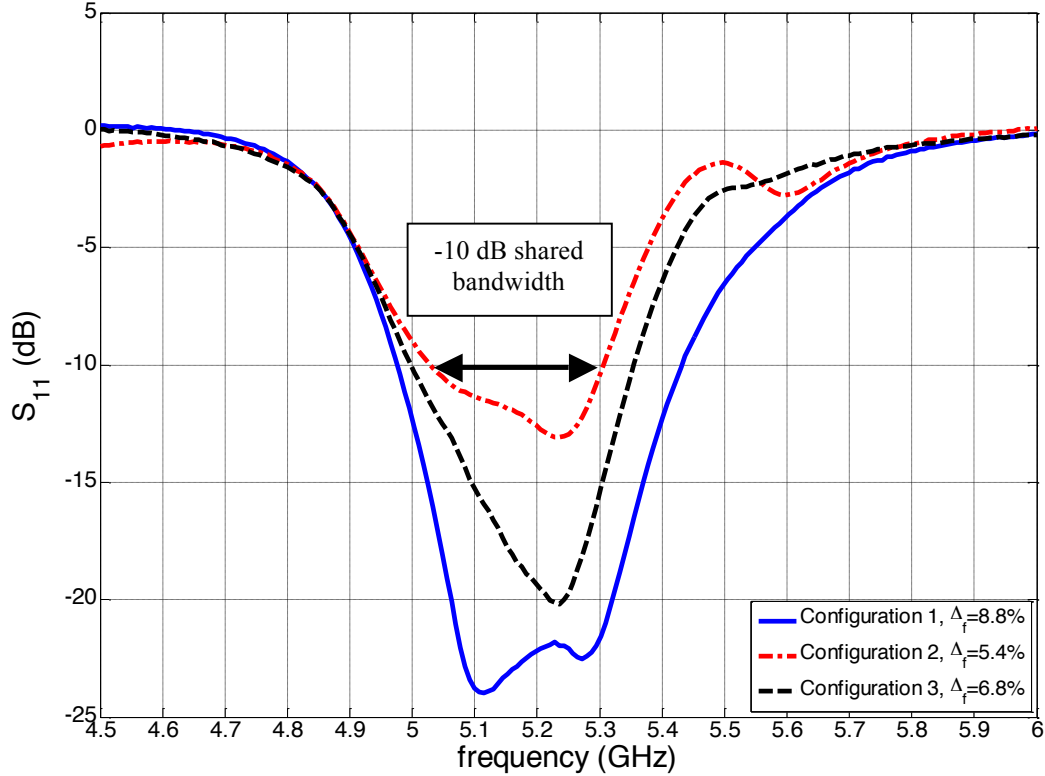


**Fig. 11 - Reflection coefficient of the build antenna in the three pattern configurations**

Measured radiation patterns for the three configurations are given in Fig. 12. Like in simulation results, gains are drawn along  $\theta$  and  $\varphi$ . The operating frequency is 5.2 GHz. Measurements have been done in a near-field anechoic chamber. Then a near-field/far-field transformation has provided the field components along  $\theta$  and  $\varphi$  in a  $4\pi$  steradian range. As in simulation, maximum gain levels are quite similar along both polarizations. Radiation reconfiguration is clearly achieved and pattern shapes are in good agreement with simulations. Differences between the simulation and the measurement are mainly assigned to the diodes. In fact, simulation did not take into account diodes which were modeled by metallic “hard-wires”. Since in practice diodes in the ON state are not perfect short-circuits, the field radiated through a short-circuited slot is not null; neither are diodes in the OFF state perfect open-circuits, therefore losses are inserted.

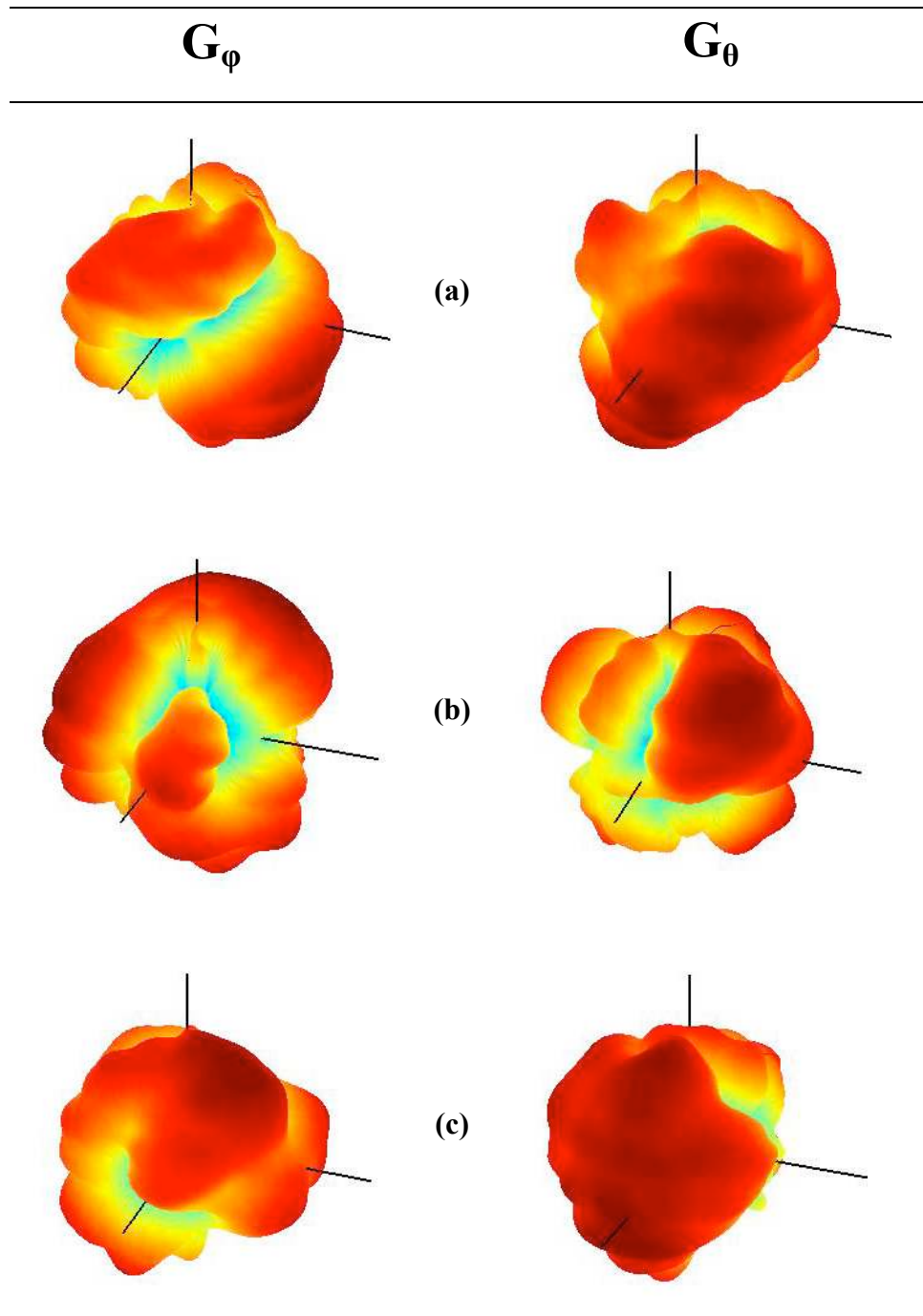


**Fig. 12 - Measured radiation patterns along  $\varphi$  (on left) and  $\theta$  (on right) for (a) configuration 1, (b) configuration 2 and (c) configuration 3**

To quantify the radiation reconfiguration effect, the envelope correlation is calculated in the next section. Performances of simulations and measurements are compared.

#### IV DIVERSITY PERFORMANCE RESULTS

The envelope correlation  $\rho_e$  provides a measure of antenna diversity performances. The lower the correlation, the better the diversity performance. This coefficient is defined as in [1]:

$$\rho_e = \frac{\left| \int_{\Omega} (XE_{1\theta}(\Omega)E_{2\theta}^*(\Omega)p_{\theta}(\Omega) + E_{1\varphi}(\Omega)E_{2\varphi}^*(\Omega)p_{\varphi}(\Omega)) d\Omega \right|^2}{\int_{\Omega} (XE_{1\theta}(\Omega)E_{1\theta}^*(\Omega)p_{\theta}(\Omega) + E_{1\varphi}(\Omega)E_{1\varphi}^*(\Omega)p_{\varphi}(\Omega)) d\Omega \int_{\Omega} (XE_{2\theta}(\Omega)E_{2\theta}^*(\Omega)p_{\theta}(\Omega) + E_{2\varphi}(\Omega)E_{2\varphi}^*(\Omega)p_{\varphi}(\Omega)) d\Omega}, \quad (2)$$

where  $E_{1\theta}$ ,  $E_{1\varphi}$ ,  $E_{2\theta}$ ,  $E_{2\varphi}$  are complex electric fields along  $\varphi$  and  $\theta$  radiated by the antenna in pattern configuration 1 and 2. The parameter  $X$  is the cross-polarization discrimination (XPD) of the incident field and is defined as  $XPD = S_{\theta}/S_{\varphi}$  (where  $S_{\theta}$  and  $S_{\varphi}$  represent the average power along the spherical coordinates  $\theta$  and  $\varphi$ ). The angle  $\Omega$  is defined by  $\theta [0:\pi]$  in elevation and  $\varphi [0:2\pi]$  in azimuth.  $p_{\theta}$  and  $p_{\varphi}$  are the Angle-of-Arrival (AoA) distributions of incoming waves.

The envelope correlation has been calculated from simulated and measured radiation patterns. Results are given versus  $XPD$  in Fig. 13 for a uniform distribution of AoA. Since the reconfigurable cubic antenna has three available pattern configurations, three envelope correlations are calculated:  $\rho_{e12}$ ,  $\rho_{e13}$  and  $\rho_{e23}$ . However, for correlations determined from simulated patterns, only one result is given because the antenna geometry is perfectly symmetric and so the three configurations are strictly identical, the only change is the  $120^\circ$  rotation. Envelope correlations  $\rho_{e12}$ ,  $\rho_{e13}$  and  $\rho_{e23}$  are consequently equal.

For envelope correlations calculated from simulated radiation patterns, two different results are given in Fig. 13. The first one is determined from the cube with ideal switches (“hard-wired” switches) whereas the second one is based on the cube with realistic switches (RF equivalent circuits). In the first case, the envelope correlation is always lower than 0.12 whereas in the second case, the envelope correlation is higher than 0.15 for  $XPD < -10$  dB. The maximum is 0.16 at  $XPD = -20$  dB. This difference can be explained by the fact that the PIN diodes do not act like perfect switches. In fact, when a diode is ON, the associated slot still radiates a small amount of power whereas with a “hard-wired” instead of an ON diode, the radiated power is null. Therefore the pattern reconfiguration is less effective. Since in practice the built antenna is not perfectly symmetrical around its main axis, envelope correlations between the three different radiation pattern configurations are not identical. The correlation between the configuration 2 and 3 is very close to the simulated one. However, other correlations are higher. As an example, for  $XPD = 0$  dB, the envelope correlation in

simulation is  $\rho_e = 0.08$  with ideal switches and  $\rho_e = 0.11$  with realistic switches whereas in measurement, the different correlation are  $\rho_{e12} = 0.23$ ,  $\rho_{e13} = 0.31$  and  $\rho_{e23} = 0.12$ . The worst envelope correlation is between pattern configurations 1 and 3 ( $\rho_{e13}$ ) and is always less than 0.35 for all XPD values. Even if  $\rho_e$  must be as low as possible, an effective diversity action can be obtained as long as  $\rho_e$  is less than 0.7 [15], [16]. These results show that the reconfigurable cubic antenna is well suited for diversity applications.

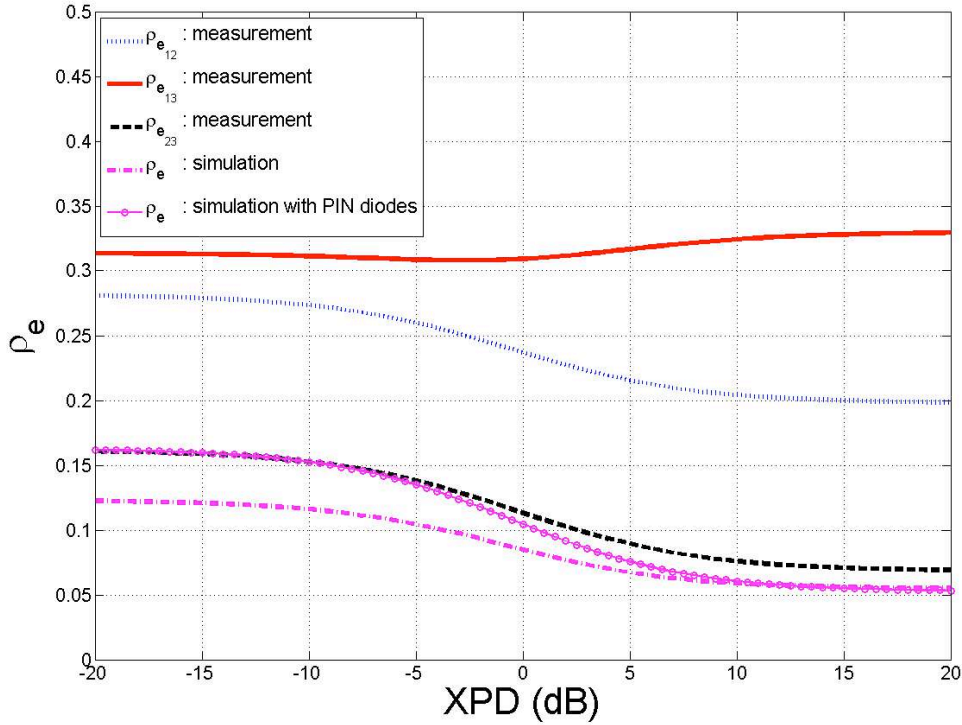


**Fig. 13 - Correlation of simulated and measured radiation patterns**

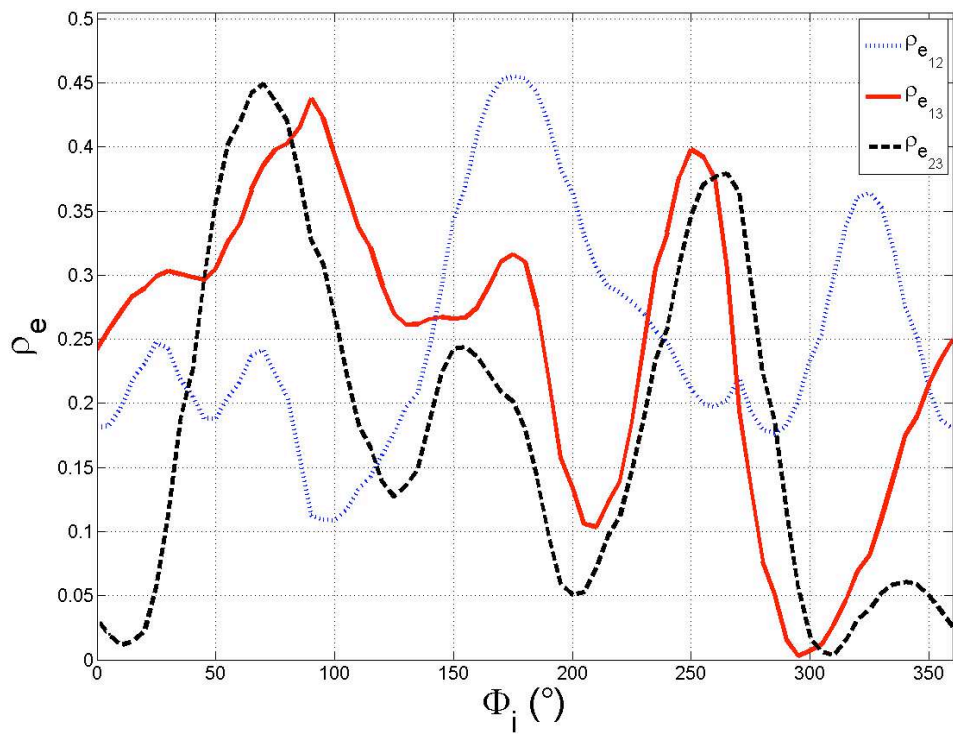
The envelope correlation is strongly dependent on the propagation properties represented in the equation (2) by the distribution of AoA  $p_\theta$  and  $p_\varphi$ . That is why results with a non-uniform distribution of AoA are also shown here. Some measurements have been done in [17] which show that the power azimuth spectrum can be well modelled with a Laplacian function. This distribution is expressed as:

$$p_\theta(\varphi) = p_\varphi(\varphi) = \frac{1}{\sigma\sqrt{2}} \exp\left(-\frac{|\varphi - \varphi_0|\sqrt{2}}{\sigma}\right), \quad (3)$$

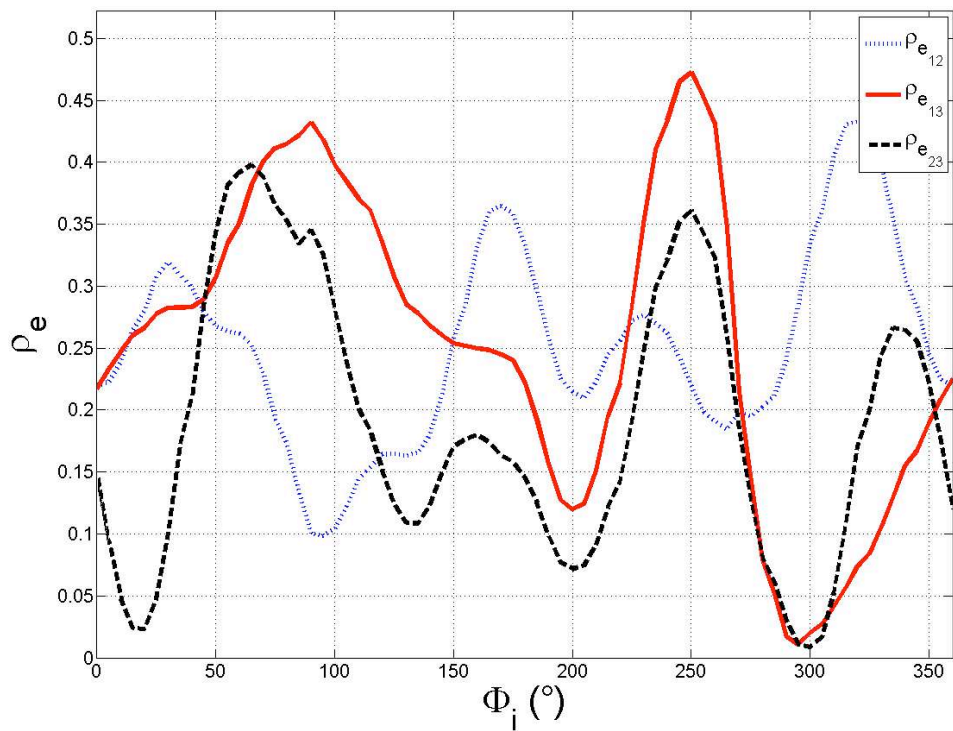
where  $\varphi_i$  is the mean of the direction of incoming waves and  $\sigma$  is the standard deviation. The elevation spectrum is assumed uniform:  $p_\theta(\theta) = p_\varphi(\theta) = 1$ .

Envelope correlations calculated from radiation patterns measured in the  $4\pi$  steradian range are shown in Fig. 14 with a deviation  $\sigma = 20^\circ$ . Results are given for a XPD of 0 dB and

6 dB which represent an indoor and an urban fading environment respectively [1]. Curves are drawn versus  $\varphi_i$ . The envelope correlation between each configuration strongly depends on  $\varphi_i$ . For example, for  $XPD = 0$  dB,  $\rho_{e12} = 0.36$ ,  $\rho_{e13} = 0.13$ ,  $\rho_{e23} = 0.05$  at  $\varphi_i = 200^\circ$  whereas  $\rho_{e12} = 0.11$ ,  $\rho_{e13} = 0.4$ ,  $\rho_{e23} = 0.27$  at  $\varphi_i = 100^\circ$ . To consider a Laplacian AoA distribution instead of a uniform distribution results in a higher correlation but still below 0.47. Furthermore, for every  $\varphi_i$ , there always exists two configurations which provide a correlation less than 0.27. Thus, high diversity performances are available in every propagation scheme.



(a)



(b)

**Fig. 14 - Envelope correlation with a Laplacian AoA distribution for**

**(a) XPD = 0 dB and (b) XPD = 6 dB**

## V CONCLUSION

The cubic cavity antenna demonstrates a new kind of reconfigurable antenna for diversity systems. This antenna concept has the potential to provide three uncorrelated radiation patterns with a single port. Each pattern configuration radiates in a  $4\pi$  steradian range and is sensitive to polarizations along  $\theta$  and  $\phi$ . These properties make such an antenna well-suited to maximize the received power in an urban or indoor environment where signals come from many different Angles-of-Arrival with arbitrary polarizations. However, because of the quasi-omnidirectional pattern, some precautions must be taken when the antenna is mounted on a structure to benefit from its interesting performances.

The use of ON/OFF switches allows a simple control command to change the pattern configuration. Although simulated radiation patterns presented in this paper assume “hard-wired” switches, similar pattern shapes have been obtained in measurement when the antenna integrates PIN diodes.

With a physical approach which has highlighted the dual resonances behavior (the cavity resonance and the slot resonance), the frequency bandwidth has been improved compared to the use of only one resonance. Thus, the -10 dB return-loss allows the antenna to be used in wireless applications operating in the 5.15 GHz – 5.35 GHz band.

Finally, envelope correlation coefficients have been calculated from simulated and measured radiation patterns. The results obtained show a low correlation between each radiation configuration which indicates that the reconfigurable cubic antenna is well-suited for diversity communications.

## ACKNOWLEDGEMENT

The authors would like to thank J.M. Floch of the “Institut d’Electronique et de Telecommunication de Rennes” for his assistance for the use of the near-field anechoic chamber.

## REFERENCES

- [1] R.G. Vaughan and J.B. Anderson, “Antenna diversity in mobile communication”, *IEEE Trans. Veh. Technol.*, vol. VT-36, pp. 149-172, Nov. 1987

- [2] J.L. Glaser and L.P. Faber, "Evaluation of polarization diversity performance", *IEEE Proceedings of the IRE*, vol. 41, pp. 1774-1778, Dec. 1953
- [3] W. Lee and Y. Yu, "Polarization diversity system for mobile radio", *IEEE Trans. Communications*, vol. 20, pp. 912-923, Oct. 1972
- [4] S. Kozono, T. Tsuruhara and M. Sakamoto, "Base station polarization diversity reception for mobile radio", *IEEE Trans. Veh. Technol.*, vol. VT-33, pp. 301-306, Nov. 1984
- [5] R.G. Vaughan and J.B. Anderson, "Polarization diversity in mobile communication", *IEEE Trans. Veh. Technol.*, vol. VT-39, pp. 177-186, Aug. 1990
- [6] R.U. Nabar, H. Bölcskei, V. Erceg, D. Gesbert and A.J. Paulraj, "Performance of multiantenna signaling techniques in the presence of polarization diversity", *IEEE Trans. Signal Process.*, vol. 50, pp. 2553-2562, Oct. 2002
- [7] H.R. Chuang and L.C. Kuo, "3-D FDTD design analysis of a 2.4 GHz polarization-diversity printed dipole antenna with integrated balun and polarization-switching circuit for WLAN and wireless communication applications", *IEEE Trans. Micro. Theory Tech.*, vol. 51, pp. 374-381, Feb. 2003
- [8] N.L. Scott, M.O. Leonard-Taylor and R.G. Vaughan, "Diversity gain from a single-port adaptive antenna using switched parasitic elements illustrated with a wire and monopole prototype", *IEEE Trans. Antennas and Propagation*, vol. 47, pp. 1066-1070, June 1999
- [9] M.A. Jensen and J.W. Wallace, "A review of antennas and propagation for MIMO wireless communications", *IEEE Trans. Antennas and Propagation*, vol. 52, pp. 2810-2824, Nov. 2004
- [10] B.A. Cetiner, H. Jafarkhani, J-Y. Qian, H.J. Yoo, A. Grau and F. DeFlaviis, "Multifunctional reconfigurable MEMS integrated antennas for adaptive MIMO systems", *IEEE Communications Mag.*, vol. 42, Issue 12, pp. 62-70, Dec. 2004

- [11] B.A. Cetiner, E. Akay, E. Sengul and E. Ayanoglu, "A MIMO system with multifunctional reconfigurable antennas", *IEEE Ant. Wirel. Propa. Lett.*, vol. 5, pp. 463-466, Sept. 2006
- [12] T.L. Roach, G.H. Huff and J.T. Bernhard, "Enabling high performance wireless communication systems using reconfigurable antennas", *Military Communications Conference MILCOM 2006*, Oct. 2006
- [13] M.D. Migliore, D. Pinchera and F. Schettino, "Improving channel capacity using adaptive MIMO antennas", *IEEE Trans. Antennas and Propagation*, vol. 54, pp. 3481-3489, Nov. 2006
- [14] J. Sarrazin, Y. Mahé, S. Avrillon and S. Toutain, "Multibeam and orthogonal polarization antenna", *European Conference on Antennas and Propagation*, 6-10 Nov. 2006
- [15] J.N. Pierce and S. Stein, "Multiple diversity with nonindependent fading", *Proc. IRE*, vol. 48, pp. 89-104, Jan. 1960
- [16] W.C. Jakes, Ed., *Microwave Mobile Communications*. New York: Wiley, 1974
- [17] K.I. Pedersen, P.E. Mogensen and B.H. Fleury, "Spatial channel characteristics in outdoor environments and their impact on BS antenna system performance", *Vehicular Technology Conference*, vol. 2, pp. 719-723, 18-21 May 1998